

Laser-shocked calcium difluoride (CaF₂) as a warm dense matter

Cite as: Phys. Plasmas **27**, 030701 (2020); <https://doi.org/10.1063/1.5135596>

Submitted: 07 November 2019 . Accepted: 10 February 2020 . Published Online: 02 March 2020

Hua Shu, Youjun Zhang , Bihan Wang , Wenge Yang , Hongliang Dong, Tsubasa Tobase, Junjian Ye, Xiuguang Huang, Sizu Fu , Qiang Zhou, and Toshimori Sekine



View Online



Export Citation



CrossMark

AVS Quantum Science

Co-Published by



RECEIVE THE LATEST UPDATES



Laser-shocked calcium difluoride (CaF₂) as a warm dense matter

HPSTAR
912-2020

Cite as: Phys. Plasmas **27**, 030701 (2020); doi: [10.1063/1.5135596](https://doi.org/10.1063/1.5135596)

Submitted: 7 November 2019 · Accepted: 10 February 2020 ·

Published Online: 2 March 2020



View Online



Export Citation



CrossMark

Hua Shu,¹ Youjun Zhang,² Bihan Wang,³ Wenge Yang,³ Hongliang Dong,³ Tsubasa Tobase,³ Junjian Ye,¹ Xiuguang Huang,¹ Sizu Fu,¹ Qiang Zhou,⁴ and Toshimori Sekine^{3,5,a)}

AFFILIATIONS

¹Shanghai Institute of Laser Plasma, Shanghai 201800, China

²Institute of Atomic and Molecular Physics, Sichuan University, Chengdu 610065, China

³Center for High Pressure Science & Technology Advanced Research, Shanghai 201203, China

⁴State Key Laboratory of Explosion Science and Technology, Beijing Institute of Technology, Beijing 100081, China

⁵Graduate School of Engineering, Osaka University, Suita 565-0671, Japan

^{a)} Author to whom correspondence should be addressed: toshimori.sekine@hpstar.ac.cn

ABSTRACT

We determined the shock equation of state of CaF₂ at pressures of ~ 0.4 – 1.5 TPa using high-power laser shock techniques. The shock velocity-particle velocity was approximated by the universal Hugoniot relationship known to metallic fluids. Our results do not support the incompressible behavior above ~ 100 GPa claimed previously. Warm dense CaF₂ is a bonded liquid above the melting point and approaches an ideal fluid above ~ 1 TPa. The measured reflectivity change of CaF₂ at the shock front, similar to the other semiconducting liquids in the warm dense region, suggests a gradual metallization process due to the presence of delocalized electrons at high shock-front temperatures.

Published under license by AIP Publishing. <https://doi.org/10.1063/1.5135596>

Calcium difluoride is a stable mineral called fluorite and has been studied intensively due to its technological applications in optics and electronics. Fluorite becomes superionic at high temperatures (>1430 K)¹ before melting at ambient pressure, and the superionic phase extends to high pressures of several GPa.² At high pressures, fluorite undergoes a phase transition to a cotunnite-structure phase at ~ 10 GPa, which also becomes superionic at high temperatures,³ and the phase transition increases the coordination number (CN) from eight to nine. Another high-pressure phase of an In₂Ni structure with CN = 11 has been known experimentally above 72 GPa at room temperature.³ Shock Hugoniot data on fluorite indicate that it is uniquely anisotropic at low shock pressures⁴ and incompressible at pressures of 100–250 GPa,⁵ respectively. There are no further data available at higher shock pressures. However, Hugoniot data up to 950 GPa from flier plate experiments using a two-stage gas gun and Z-machine were presented recently.⁶

High-pressure studies and theoretical considerations^{7,8} suggest similar behavior in the AX₂ compounds represented by SiO₂ (Ref. 5). SiO₂ undergoes a series of phase transitions to coesite (CN = 4), stishovite (CN = 6), CaCl₂-type (CN = 6), α -PbO₂-type (CN = 6), and pyrite-type (CN = 8) structures with increasing pressure and has been predicted to be cotunnite (CN = 9) and Fe₂P-type (CN = 9) structures

above 650 GPa. Experimental data on CaF₂ may have implications for the high-pressure candidates in the AX₂ compounds because fluorite has CN = 8 in the ambient state and undergoes phase transitions, including a cotunnite structure at ~ 10 GPa. These coordination changes in solids are expected to affect the liquid structures above the melting point of the corresponding phase, and the density along the Hugoniot may be associated with such a coordination increase in liquids.

A one-component plasma model can describe its equilibrium and near-equilibrium properties by a single parameter called the Coulomb coupling parameter Γ , a ratio of the mean potential energy per particle to the mean kinetic energy.⁹ The mean particle energy per particle is q^2/a , where q and a are the electric charge and Wigner–Seitz radius, respectively. The mean kinetic energy is $k_B T$, where k_B and T are the Boltzmann constant and temperature, respectively. As Γ increases, the system changes from a nearly collisionless, gaseous state ($\Gamma \ll 1$), through increasing correlated, fluid-like media ($\Gamma \approx 50$), to a first-order fluid-like phase ($\Gamma > 175$). Therefore, it is expected that metals such as Be, Al, Fe, Cu, and Mo behave like the universal Hugoniot of fluid metals (UHFM) in the shock velocity (U_s km/s)-particle velocity (U_p km/s) plot,¹⁰ given by $U_s = 5.8 + 1.2U_p$. The relation is extendable to some oxide systems (SiO₂ and Gd₃Ga₅O₁₂)¹¹

above a critical pressure of 300–400 GPa although there are some exceptions.¹¹ It is interesting to check this relation in fluoride systems at warm dense matter conditions because different interactions between oxides and fluorides are expected in their warm dense states. We investigated the principal Hugoniot of fluorite above 400 GPa where it becomes warm dense matter and is reflective under shock compression because it is expected to undergo metallization in CaF₂ at 210 GPa.¹² However, recent calculations predicted much higher metallization pressures.^{13,14} A region for warm dense matter can be characterized by materials with densities similar to solids at high temperatures above a few eVs, which is generated by shock compressions at pressures above several hundred GPa.

Our experiments were performed at the National Laboratory on High Power Laser and Physics using the Shenguang-II (SG-II) Nd:glass laser. We used four beams bundled in an F/3.5 cone angle and smoothed by the lens-arrays system at 351 nm (third harmonics of the SG-II:3 ω). The temporal behavior of the laser pulse was approximated as a square shape with a full width at half maximum (FWHM) of 1.0 ns and a rise and fall time of 100 ps each. The laser beams were focused onto the target with a diameter of $\sim 500 \mu\text{m}$.

A single crystal CaF₂ (density of 3.186 g/cm^3)⁴ was cut and polished into pieces ($4 \times 2 \times 0.2 \text{ mm}$). Quartz (a well calibrated standard) was used as the reference to determine the Hugoniot and set parallel on aluminum ($30 \mu\text{m}$ thick) foil. CH foil ($30 \mu\text{m}$ thick) and thin gold ($1.5 \mu\text{m}$ thick) were used as the ablator and x-ray shield, respectively. The target assemblage is illustrated schematically in Fig. 1.

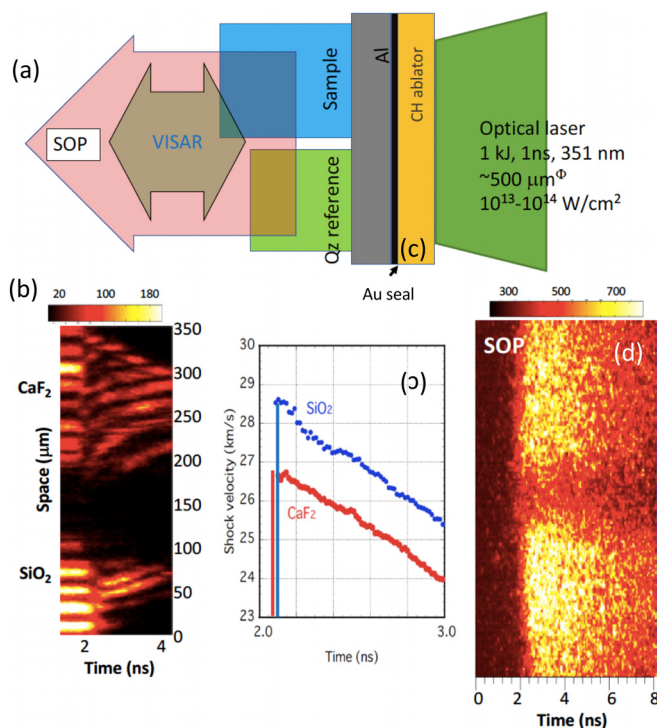


FIG. 1. Schematic illustration of target used in the present laser shock study (a), typical VISAR (b), calculated shock velocity (c), and streaked optical pyrometer (SOP) (d).

We used standard diagnostics to measure the shock velocity and thermal emission from the shock front simultaneously^{15,16} because single crystal CaF₂ is transparent at ambient condition. Our line-imaging VISARs consisted of two different constants of velocity per fringe (3.87 km/s/Fr and 1.85 km/s/Fr for quartz and 3.95 km/s/Fr and 1.88 km/s/Fr for CaF₂, respectively) to get a shock velocity at the reflective surface. The probe laser of the VISAR system was a 50 ns pulse with a wavelength of 660 nm. In our experiments, the driven pressures were sufficient to produce optically reflective shock fronts in both quartz and CaF₂ samples. This resulted in direct, time-resolved measurements of the shock velocity in both samples of quartz and CaF₂. After determining the shock velocities (U_s km/s) of CaF₂ and SiO₂ simultaneously, the impedance match method¹⁷ was applied to calculate the particle velocity (U_p km/s) of CaF₂ through the mirror reflection of the principle Hugoniot of aluminum. We used glue to assemble the targets. We assumed equilibrium among Al, glue, and CaF₂/SiO₂ because the VISAR fringes were disturbed in the glue and subject to significant decay and took the shock velocity at the front surface to apply the impedance match method. Then, the pressure and density for CaF₂ were calculated using the Rankine–Hugoniot relations. Thermal emission was recorded as a streaked optical pyrometer (SOP) at a wavelength of 442 nm with a narrow band (FWHM) of 30 nm, and reflectivity (r) was estimated through the changes of VISAR signals relative to that of Al. The method of calibration and error estimation of the SOP was similar to that described by Miller *et al.*¹⁸ and Gregor *et al.*¹⁹ In shot #3 (Table I), the emission was observed without the narrow band filter and the temperature was not calculated. The emissivity (ϵ) was estimated using the relation of $r + \epsilon = 1$. The temperature was checked against the quartz temperature data.²⁰

The experimental data are summarized in Table I. Figure 2 illustrates the relationships between shock velocity (U_s km/s) and particle velocity (U_p km/s) and between pressure (P GPa) and density (d g/cm³) for fluorite. The U_s - U_p relation is approximated linearly as $U_s = 8.92(\pm 0.57) + 0.98(\pm 0.04)U_p$ and is compared with the results in the study by Root *et al.* (marked by the green dotted line) and a model of the universal Hugoniot U_s - U_p relation as metallic fluids^{10,11} marked by the red broken line. They are all in good agreement with a small slope variation. Our data indicate a possible connection to an extension of the data⁵ in terms of both U_s - U_p and P - d . In the P - d relation, the possible trend as an incompressible CaF₂ behavior at pressures of $\sim 100 \text{ GPa}$ – 250 GPa ⁵ is not supported by our data although the shock Hugoniot data up to 950 GPa⁶ and the static compression data at room temperature³ do not indicate an incompressible behavior. The present Hugoniot P - d relation, however, is more compressible than that by Root *et al.*⁶ and can be extendable from the data points.⁵ If it is the case, CaF₂ may maintain almost constant density during the melting process at pressures of $\sim 100 \text{ GPa}$ – $\sim 300 \text{ GPa}$ and starts to increase the density after complete melting about 300–400 GPa. This seems to differ from the results⁶ that indicate a monotonous increase in density during melting. This difference may occur at different melting kinetics due to different strain rates. We need further study to explain it.

The reflectivity based on the present VISAR measurements using a wavelength of 660 nm is determined for quartz and CaF₂ and listed in Table I. A comparison with the previous studies on quartz^{22,23} indicates our data on quartz are very similar, and the reflectivity of CaF₂ is similar to that of quartz at pressures below $\sim 1 \text{ TPa}$ and significantly

TABLE I. Experimental results on CaF₂ referenced by quartz in the present study. The $U_s(\text{Al})$ - $U_s(\text{Qz})$ relation on the principal Hugoniot was determined by Hicks *et al.*²⁰ The quartz Hugoniot is cited from Desjarlais *et al.*²¹ The values in parentheses are errors. There was no narrow band filter in shot #3, and the results in shot #1316 were combined in two shots at an energy in which VISAR data were obtained for quartz and CaF₂ separately.

Shot No.	Energy (J)	U_s (Qz) (Km/s)	U_p (km/s)	Pres (GPa)	Density (g/cm^3)	Temp (K)	Refl	U_s (CaF ₂) (Km/s)	U_p (km/s)	Pres (GPa)	Density (g/cm^3)	Temp (K)	Refl
3	1026	28.72 (0.37)	18.73 (0.48)	1426 (53)	7.62 (0.35)	...	0.48 (0.06)	26.73 (0.31)	18.16 (0.83)	1542 (75)	9.89 (0.34)	...	0.32 (0.04)
4	929	24.90 (0.43)	15.67 (0.47)	1034 (48)	7.15 (0.34)	64000 (11500)	0.46 (0.05)	23.30 (0.32)	15.35 (0.93)	1138 (71)	9.32 (0.39)	44600 (8000)	0.27 (0.04)
7	875	21.34 (0.50)	12.87 (0.48)	728 (44)	6.68 (0.31)	44000 (7500)	0.24 (0.03)	21.04 (0.46)	12.51 (1.05)	837 (72)	7.84 (0.42)	32500 (5900)	0.23 (0.03)
8	730	16.26 (0.54)	9.03 (0.47)	389 (33)	5.96 (0.28)	22500 (4100)	0.24 (0.03)	16.90 (0.50)	8.70 (1.09)	467 (60)	6.55 (0.44)	18900 (3600)	0.22 (0.03)
1316	893	24.19 (0.55)	15.11 (0.53)	969 (55)	6.98 (0.33)	23.07 (0.45)	14.73 (1.17)	1080 (89)	8.79 (0.43)

less than that of quartz at high pressures over ~ 1 TPa. There seems to be little difference by two different wavelengths used as the probing light. The temperature based on the SOP record and the emissivity are calculated from the emission counts and also listed in Table I. A comparison of the quartz temperature agrees with the previous results, and the shock temperature for CaF₂ was slightly lower than that for quartz (Table I) in a shot. These reflectivity and temperature measurements indicate that CaF₂ is a warm dense matter under the present shock conditions. The Coulomb coupling parameters (Γ) for CaF₂ and SiO₂ were calculated using the measured Hugoniot data when the Wigner-Seitz radius (a) is approximated by $\sqrt[3]{Z/(\rho A)/2}$. Z , ρ , and A are the averaged atomic weight, density, and the Avogadro's number, respectively. The estimated a is $0.90 \text{ \AA} \sim 1.0 \text{ \AA}$ for the universal Hugoniot fluid metals¹¹ and $\sim 0.85 \text{ \AA}$ for Gd₃Ga₅O₁₂ (Ref. 11) at ~ 1 TPa. It decreases from 0.94 \AA to 0.82 \AA for CaF₂ and 0.89 \AA to 0.83 \AA for SiO₂ with increasing shock pressure in the present experiments at $0.4 \text{ TPa} \sim 1.5 \text{ TPa}$. Assuming that 5% of the total number of the

electrons is delocalized in the present experiments, the estimated Γ values are calculated to be 16–44 for CaF₂ and 7–22 for SiO₂, respectively, suggesting considerably strong interparticle interactions over the present experimental conditions. The difference in reflectivity between CaF₂ and SiO₂ above ~ 1 TPa may suggest a difference in the liquid structure as supported by the estimated Γ values.

In Fig. 3, the calculated reflectivity is shown for comparison. The shock front reflectivity was calculated by $r = [(n - n_0)/(n + n_0)]^2$, where n and n_0 are the refractive index at the shock front and 1.43 (ambient index of CaF₂). We used a similar method to Hicks *et al.*²⁴ and Celliers *et al.*²⁵ to fit the energy gap in the electron density of state (E_g) and $\gamma = \tau/\tau_{\text{min}}$, where τ and τ_{min} are the electron relaxation time and the

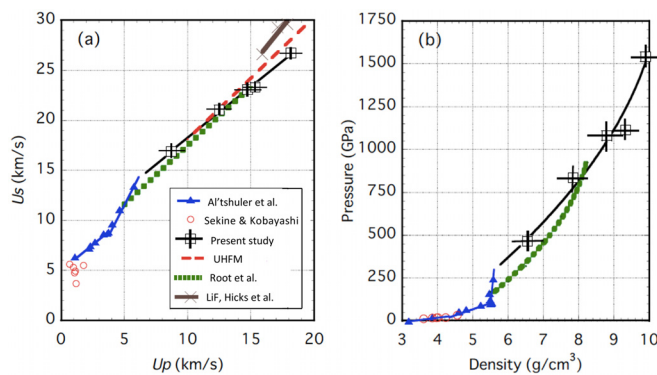


FIG. 2. Hugoniot relationships for CaF₂ between shock velocity (U_s km/s) and particle velocity (U_p km/s) (a) and between pressure (GPa) and density (g/cm^3) (b). Present data are black squares with errors. The blue triangles represent Al'tshuler *et al.*,⁵ green dotted lines are Root *et al.*,⁶ red broken line in (a) is the universal U_s - U_p relation for fluid metals,^{10,11} and red circles are Sekine and Kobayashi.⁴ The brown line at the right top in (a) represents the results for LiF (Ref. 24).

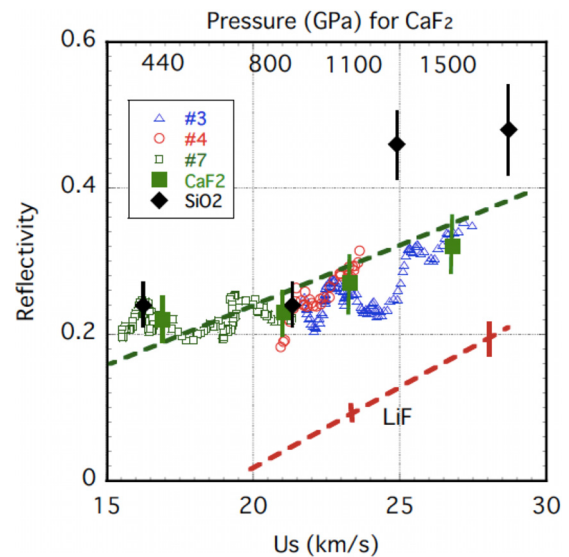


FIG. 3. Measured reflectivity of CaF₂ as a function of shock velocity (U_s km/s) and pressure (GPa) in three shots. Solid squares and diamond are reflectivities on the Hugoniot of CaF₂ and SiO₂ in the present study (Table I). The green broken and brown broken lines represent the calculated reflectivities for CaF₂ and LiF (Ref. 24), respectively, based on a model described by Hicks *et al.*²⁴ and Celliers *et al.*²⁵ The fitting parameters of E_g and γ were obtained to be 4 eV and 0.85 for CaF₂.

minimum scattering time, respectively. There is a good agreement, but the gap closure changes gradually, not suddenly by pressure.

The bandgap of CaF₂ is known to be ~ 10 eV²⁶ and smaller than that of LiF (~ 14 eV²⁴). We compare the Hugoniot and reflectivity between CaF₂ and LiF. The three data points for LiF at pressures of 1.1–1.4 TPa²⁴ are compared in Figs. 2 and 3. The U_s - U_p plot locates slightly above the universal relation for the fluid metals approximated by $U_s = 5.90 + 1.22 U_p$ with a few percent variations in U_s at a given U_p (Ref. 11). The estimated values of a and Γ for LiF are 0.75 Å and 5, respectively. This suggests that LiF may have weaker interactions in the warm dense matter state and higher metallization pressure than CaF₂. There is no consensus on the estimated metallization pressures, but the most recent calculations predict them to be 2.25 TPa¹⁴ for CaF₂ and above 4 TPa²⁷ for LiF. Based on the VISAR measurements, the shock front with elevated temperature produces delocalized electrons and becomes a semiconductor. The thermally activated process is a gradual change dependent on the shock strength, but it differs from the sudden metallization by pressure. The gradual reflectivity change may provide information on the liquid properties. We calculated reflectivities for CaF₂ using a simple model described by Hicks *et al.*²⁴ and Celliers *et al.*,²⁵ as shown in Fig. 3. If we refer to the results on shocked quartz, as investigated the most intensively and thought to be a bonded liquid at 0.25–0.65 TPa, there is a dissociation of molecular bonds at 0.65–1 TPa, and it is a simple fluid above 1 TPa.^{28,29} CaF₂ is expected to behave like a simple fluid at pressures above 1.5 TPa because of a typical ionic crystal and more like molecules such as H₂O in the U_s - U_p relation¹⁰ (Fig. 2).

The present results on laser-shocked CaF₂ are summarized as follows:

- (1) The U_s - U_p relation in the warm dense matter state is approximated as the universal Hugoniot for fluid metals, but it may be little affected by different interactions among different components.
- (2) The incompressibility above ~ 100 GPa, claimed previously, is not confirmed in the present study.
- (3) The melting of CaF₂ during shock compression needs further studies to take into account the strain rate.
- (4) The shock front above ~ 0.4 TPa becomes a semiconductor and displays a similar behavior to quartz.

We thank the laser operation team for their help. This project was supported by the science challenge project, China (Grant No. TZ2017001). T. Sekine acknowledges partial support from the National Natural Science Foundation of China (NSFC No. 41974099). Y. J. Zhang acknowledges financial support from the National Key Laboratory of Shock Wave and Detonation Physics (No. 6142A03182006) and the Fundamental Research Funds for the Central Universities (No. YJ201809). Freyja O'Toole read and improved our final draft. Two reviewers made very helpful comments to complete this manuscript.

REFERENCES

- ¹L. L. Boyer, *Phys. Rev. Lett.* **45**, 1858 (1980).
- ²C. Cazorla and D. Errandonea, *Phys. Rev. Lett.* **113**, 235902 (2014).
- ³S. M. Dorfman, F. Jiang, Z. Mao, A. Kubo, Y. Meng, V. B. Prakapenka, and T. S. Duff, *Phys. Rev. B* **81**, 174121 (2010).
- ⁴T. Sekine and T. Kobayashi, *Phys. Chem. Miner.* **38**, 305 (2011).
- ⁵L. V. Al'tshuler, M. A. Podurets, G. V. Simakov, and R. F. Trunin, *Phys. Solid State* **15**, 969 (1973).
- ⁶S. Root, W. Desjarlais, R. Lemke, P. Kalita, and S. Alexander, Sandia Report No. SAND2018-0182C 659805 (2018).
- ⁷J. R. Nelson, R. J. Needs, and C. J. Pickard, *Phys. Rev. B* **95**, 054118 (2017).
- ⁸T. Tsuchiya and J. Tsuchiya, *Proc. Natl. Acad. Sci. U. S. A.* **108**, 1252 (2011).
- ⁹M. Baus and J. P. Hansen, *Phys. Rep.* **59**(1), 1 (1980).
- ¹⁰W. J. Nellis, *Shock Compression of Condensed Matters-2005*, edited by M. D. Furnish, M. Elert, T. P. Russell, and C. T. White (American Institute of Physics, 2006), pp. 115–118.
- ¹¹N. Ozaki, W. J. Nellis, T. Mashimo, M. Ramzan, R. Ahuja, T. Kaewmaraya, T. Kimura, M. Knudson, K. Miyanishi, Y. Sakawa, T. Sano, and R. Kodama, *Sci. Rep.* **6**, 26000 (2016).
- ¹²V. Kanchana, G. Vaitheesmaran, and M. Rajagopalan, *Physica B* **328**, 283 (2003).
- ¹³X. Wu, S. Qin, and Z. Wu, *Phys. Rev. B* **73**, 134103 (2006).
- ¹⁴S. Cui, W. Feng, H. Hu, Z. Feng, and Y. Wang, *Comp. Mater. Sci.* **47**, 41 (2009).
- ¹⁵T. Sekine, N. Ozaki, K. Miyanishi, Y. Asaumi, T. Kimura, B. Albertazzi, Y. Sato, Y. Sakawa, T. Sano, S. Sugita, T. Matsui, and R. Kodama, *Adv. Sci.* **2**, e1600157 (2016).
- ¹⁶H. Shu, X. Huang, H. Pan, J. Ye, F. Zhang, G. Jia, Z. Feng, Y. Tu, Z. Xie, and S. Fu, *Int. J. Fract.* **206**, 81 (2017).
- ¹⁷P. M. Celliers, G. W. Collins, D. G. Hicks, and J. H. Eggert, *J. Appl. Phys.* **98**, 113529 (2005).
- ¹⁸J. E. Miller, T. R. Boehly, A. Melchior, D. D. Meyerhofer, P. M. Celliers, J. H. Eggert, D. G. Hicks, C. M. Sorce, J. A. Oertel, and P. M. Emmel, *Rev. Sci. Instrum.* **78**, 034903 (2007).
- ¹⁹M. C. Gregor, R. Boni, A. Sorce, J. Kendrick, C. A. McCoy, D. N. Polzin, T. R. Boehly, P. M. Celliers, G. W. Collins, D. E. Fratanduono, J. H. Eggert, and M. Millot, *Rev. Sci. Instrum.* **87**, 114903 (2016).
- ²⁰D. G. Hicks, T. R. Boehly, P. M. Celliers, J. H. Eggert, E. Vianello, D. D. Meyerhofer, and G. W. Collins, *Phys. Plasma* **12**, 082702 (2005).
- ²¹M. P. Desjarlais, M. D. Knudson, and R. Cochrane, *J. Appl. Phys.* **122**, 035903 (2017).
- ²²D. G. Hicks, T. R. Boehly, J. H. Eggert, J. E. Miller, P. M. Celliers, and G. W. Collins, *Phys. Rev. Lett.* **97**, 025502 (2006).
- ²³T. Qi, M. Millot, R. G. Kraus, S. Root, and S. Hamel, *Phys. Plasma* **22**, 062706 (2015).
- ²⁴D. G. Hicks, P. M. Celliers, G. W. Collins, J. H. Eggert, and S. J. Moon, *Phys. Rev. Lett.* **91**, 035502 (2003).
- ²⁵P. M. Celliers, P. Loubeyre, J. H. Eggert, S. Brygoo, R. S. McWilliams, D. G. Hicks, T. R. Boehly, R. Jeanloz, and G. W. Collins, *Phys. Rev. Lett.* **104**, 184503 (2010).
- ²⁶R. A. Heaton and C. C. Lin, *Phys. Rev. B* **22**, 3629 (1980).
- ²⁷D. E. Fratanduono, T. R. Boehly, M. A. Barrios, D. D. Meyerhofer, J. H. Eggert, R. F. Smith, D. G. Hicks, P. M. Celliers, D. G. Braun, and G. W. Collins, *J. Appl. Phys.* **109**, 123521 (2011).
- ²⁸A. Denoëud, S. Mazevet, F. Guyot, F. Dorchie, J. Gaudin, A. Ravasio, E. Brambrink, and A. Benuzzi-Mounaix, *Phys. Rev. E* **94**, 031201(R) (2016).
- ²⁹M. Li, S. Zhang, H. Zhang, G. Zhang, F. Wang, J. Zhao, C. Sun, and R. Jeanloz, *Phys. Rev. Lett.* **120**, 215703 (2018).